

## The thermal state and hydrodynamics of evaporating hydrocarbon droplets. 2. Energy interpretation of sprayed n-decane evaporation process

G. Miliauskas\*, J. Talubinskas\*\*, A. Adomavičius\*\*\*, E. Puida\*\*\*\*

\*Kaunas university of technology, K.Donelaičio 20, Kaunas, 44239, Lithuania, E-mail: [gimil@ktu.lt](mailto:gimil@ktu.lt)

\*\*Kaunas university of technology, K.Donelaičio 20, Kaunas, 44239, Lithuania, E-mail: [julius.talubinskas@gmail.com](mailto:julius.talubinskas@gmail.com)

\*\*\*Kaunas university of technology, K.Donelaičio 20, Kaunas, 44239, Lithuania, E-mail: [arado@ktu.lt](mailto:arado@ktu.lt)

\*\*\*\*Kaunas university of technology, K.Donelaičio 20, Kaunas, 44239, Lithuania, E-mail: [epuida@ktu.lt](mailto:epuida@ktu.lt)

**crossref** <http://dx.doi.org/10.5755/j01.mech.18.3.1885>

### Nomenclature

$a$  - thermal diffusivity,  $m^2/s$ ;  $B_T$  - Spalding heat transfer number;  $c_p$  - specific heat,  $J/(kg\ K)$ ;  $Fo$  - Fourier number;  $k$  - conductive heating;  $k+r$  - combine heating;  $L$  - latent heat of evaporation,  $J/kg$ ;  $m$  - vapour mass flux density,  $kg/(s\ m^2)$ ;  $n$  - number of the term in infinite sum;  $q$  - heat flux density,  $W/m^2$ ;  $p$  - pressure,  $Pa$ ;  $R$  - radius of droplet,  $m$ ;  $r$  - radial coordinate,  $m$ ;  $T$  - temperature,  $K$ ;  $\eta$  - dimensionless coordinate;  $\lambda$  - thermal conductivity,  $W/(m\ K)$ ;  $\rho$  - density,  $kg/m^3$ ;  $\tau$  - time,  $s$ .

Subscript:  $e$  - equilibrium evaporation;  $g$  - gas;  $f$  - phase change;  $k$  - conductive;  $m$  - mass average;  $r$  - radiative;  $R$  - droplet surface;  $0$  - initial state.

Superscript:  $+$  - external side of a surface;  $-$  - internal side of a surface.

### 1. Introduction

A wide range of thermal technologies based on liquid dispersion are applied in different fields of modern day civilization. Searching for articles in the ISI database SIENCE DIRECT [1] by inputting the keywords "fuel droplet evaporation" around eight thousand articles that belong to this thematic group are found. In a variety of sprayed evaporating droplets, pure hydrocarbons and their mixtures can be highlighted. Numerous hydrocarbon droplet evaporation studies [1-5] indicate that the importance of knowledge about these processes is indubitable. In [5] advanced methods for studying droplet evaporation are discussed in detail. In the aforementioned methods, it is attempted to complexly evaluate the heat and mass transfer in droplets and their surroundings. Great opportunities for complex analysis are opened up due to the recent wide application [6-9] of combined analytical and numerical methods of heat and mass transfer in fluid systems modelling. In the methods mentioned above, numerical modelling schemes of unsteady evaporating droplets are constructed for the system of algebraic-integral equations. These equations are the result of analytical restructuring of a droplet's heat and mass transfer differential equations based on the initial assumption that composite heat transfer by conduction and radiation takes place in the semi-transparent droplet. The boundary conditions for combined heat and mass transfer task in this case are described by the as of yet unknown functions: droplet dimension  $R(\tau)$  and it's surface temperature  $T_R(\tau)$ . Iterative numerical solution

schemes should be applied to concretize these functions. The stability and rapid convergence of numerical solutions is essential to the operating of the numerical schemes. Specific peculiarities of numerical schemes depend on the adopted initial assumptions based on the physical nature of the solved problem. Some factors influencing the heat and mass transfer processes should be either rated or denied. Among the essential influencing factors, the following are worth noting: nonstationarity of processes, Stefan hydrodynamic flow effects on the intensity of droplet heating and evaporation rate, liquid temperature and vapour pressure changes in the Knudsen layer, the spectral selective absorption of radiation in semitransparent droplets. The detailed evaluation of droplet heat and mass transfer conditions allows us to receive the fundamental conclusions about the combined processes of dispersed liquid heating and evaporation while enabling us to highlight the essential factors which determine the intensity of the aforementioned processes. The assessment of the influence of these factors on droplets transfer processes is very important in a variety of practical aspects [9-12].

By using a combined analytical and numerical iterative method for solving the liquid droplet evaporation task, preconditions for the detailed exploration of combined heat and mass transfer interactions were established. Using this method, the essential influence of the heating conditions impact on the thermal state of evaporating droplet was investigated in [9]; the peculiarities of phase transition parameter variation in the case of simple conductive heating were highlighted in [12]. The unsteady temperature field function  $T_k(\eta, Fo)$  is the same for all given liquid droplets if the initial temperature of the droplets and their surroundings is known. Characteristic curves may be noted from the curves described by the function  $T_{k,\eta}(Fo)$ . This is primarily the curves describing variation of the temperature on the droplet's surface  $T_{k,\eta=1} = T_{k,\eta=1}(Fo)$  and its centre  $T_{k,\eta=0}(Fo)$ . Peculiarity of equilibrium evaporation regime of conductively heated droplet is:  $T_k(\eta, Fo > Fo_e) \equiv \text{const}$ . It is important to note that all heat and mass transfer parameter changes can be described by some characteristic curves when the droplets are heated conductively. It is necessary to express the desired parameter in normalized form in correspondence to the Fourier criterion. Usually, for parameter normalization, the initial state and equilibrium evaporation values are used [12]. To compile specific parameter characteristic curves for the conductively heated droplet it is sufficient to model the

evaporation process of a freely chosen droplet. Because of this, the extent of the initial numerical experiment can be significantly reduced. After the characteristic curves are calculated, all that remains is to model evaporation of the droplet in randomly chosen boundary conditions of heat exchange and to use the comparative method in order to evaluate the influence of more complicated heat transfer conditions in terms of their impact on the transfer processes interaction.

However, the factors affecting the unique conditions of evaporation of the conductively heated droplets are still not identified. In order to determine the aforementioned factors, a more detailed droplet heating and evaporation process energy content interpretation is required. In this article, the numerical investigation of the energy state of the liquid n-decane evaporating droplet by modelling in different cases of heating is presented.

## 2. Research methodology

In the first article of this series it was shown that in the medium diameter spread of the hydrocarbon droplet which is important in thermal engineering technologies, the spontaneous liquid circulation inside the droplet can be excluded. Therefore, a well-developed model of unsteady temperature field  $T_{k+r}(r, \tau)$  water droplet evaporation where the heat spread in semitransparent droplets is described by radiation and conduction, was applied in order to model n-decane droplet evaporation [8]

$$T(r, \tau) = T_R(\tau) + \frac{2}{r} \sum_{n=1}^{\infty} \sin \frac{n\pi r}{R} \times \left[ \begin{aligned} & (-1)^n \frac{R}{n\pi} \frac{dT_R}{d\tau_*} + \\ & \int_0^{\tau} \left[ \frac{1}{R\rho c_p} \int_0^R q_r (\sin n\pi\eta - n\pi\eta \cos n\pi\eta) dr \right] d\tau_* \end{aligned} \right] \times \exp \left[ -a \left( \frac{n\pi}{R} \right)^2 (\tau - \tau_*) \right] d\tau_* \quad (1)$$

In the partial case where  $q_r(r, \tau) \equiv 0$ ,  $T_{k+r}(r, \tau)$ , the function can be simplified into the function  $T_k(r, \tau)$  which describes the conductive heat spread inside the droplet.

The local radiation flux in the droplet can be described by the significantly nonlinear integral function  $q_r(\tau)$  [8]. Its numerical solution algorithm requires the function  $T_{k+r}(r, \tau)$  to be predefined to be able to calculate the spectral radiation intensity in the droplet and take into account the peculiarities of the complex refractive index  $n_{\omega k} = n_{\omega} - ik_{\omega}$  of a semitransparent liquid. The value of  $n_{\omega k}$  for n-decane is known [13]. Since the liquid n-decane absorption rate  $\kappa_{\omega}$  in the radiation spectrum is of finite size, it can be concluded that the radiation flux inside of the droplet is the same as outside of it:  $q_r^- \equiv q_r^+$ . The balance of the heat fluxes on the surface of the evaporating droplet can be described by combining  $T_{k+r}(r, \tau)$ ,  $q_r(r, \tau)$  and the steam flow-density function. When the droplet is heated by radiation and conduction, the condition of balance is described as

$$\bar{q}_{\Sigma}^+ + \bar{q}_{\Sigma}^- + \bar{q}_f \equiv \frac{\lambda_{vg}}{R} (T_g - T_R) \ln \frac{1+B_T}{B_T} - \left. -\lambda \frac{\partial T(r, \tau)}{\partial r} \right|_{r=R^-} - m_v^+ L = 0 \quad (2)$$

In this equation: steam flow is considered to be positive when the droplet is evaporating; the influence of Stefan's hydrodynamic flow on the convective heating of the droplet is assessed by Spolding's thermal parameter logarithmic function; the temperature gradient in the droplet is determined by taking Eq. (1) into consideration; the density of the vapour flux on the surface of the droplet is described according to the recommendations of [14]; finally, the influence of radiation can not be identified directly, however, it practically affects the unsteady temperature field function  $T_{k+r}(r, \tau)$ .

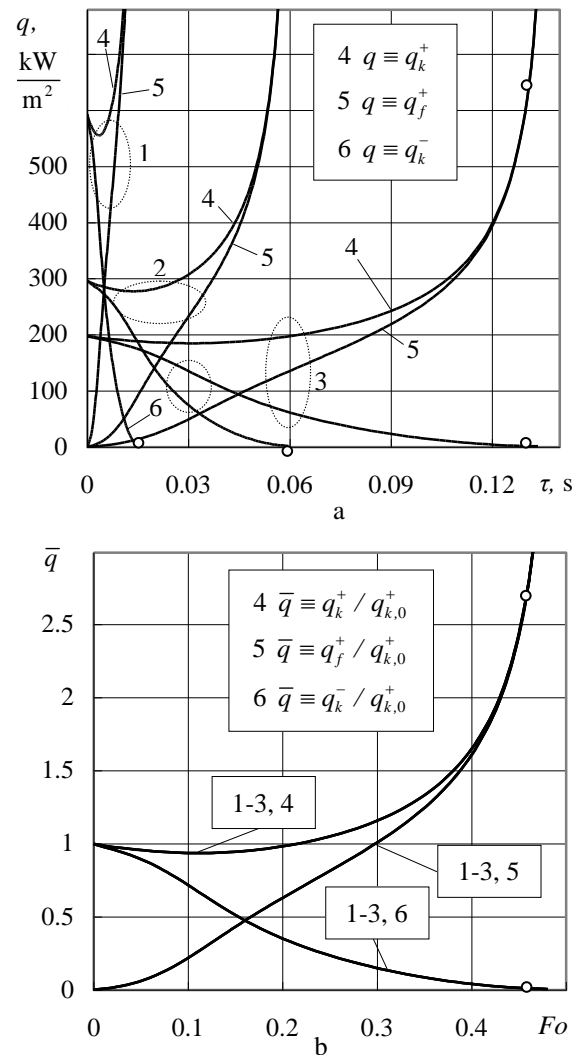


Fig. 1 Heat fluxes on the surface of the conductively heated (k) n-decane droplet: a - time is expressed in seconds; b - Fourier number.  $R$ , m: 1 - 0.00005, 2 - 0.0001, 3 - 0.00015;  $T_g = 1000$  K

Eq. (2) is solved numerically by the iterative scheme [8] based on the fastest descent method. The heat fluxes on the surface of the droplet are calculated in the freely selected moments of time  $\tau_i$ . The temperature on the surface of the droplet  $T_{R,i}$  is calculated from Eq. (2). The end condition of the iterative process is defined as permis-

sible error 0.01% of the heat flux balance on the droplet surface. After the function  $T_R(\tau)$  is determined, all desired droplet heat and mass transfer parameters  $P(\tau)$  can be calculated. Calculations are done in two cases: when droplets are heated conductively ( $P \equiv P_k$ ) or when they are heated both conductively and by radiation (combined heating) ( $P \equiv P_{k+r}$ ). After the calculations are made, a parameter comparative analysis (benchmarking) is carried out which allows us to assess the effects of combined heating.

### 3. Comparative analysis of modelling results

The evaporation of mid-size and larger n-decane droplets in temperature  $T_g$  and pressure of 0.1 MPa dry air was modelled. The impact of the Knudsen layer on the evaporation of the droplets was ignored. In the case of conductive heating it was assumed that the droplets do not move relative to the air around them. In the case of combined heating, the outside air temperature  $T_{sr} \equiv T_g$  black radiation source was assumed. The variation of the heat flux on the surface of the evaporating droplet in the cases of conductive (Fig. 1) and combined heating (Fig. 2) is very peculiar. When the initial n-decane droplet temperature and environmental parameters are the same, the heat flux functions  $\bar{q}_k^+(Fo)$ ,  $\bar{q}_f(Fo)$  and  $\bar{q}_k^-(Fo)$  in no dimensional form are identical (Fig. 2, b). This peculiarity of the evaporation of the conductively heated droplet allows obtaining the characteristic curves  $\bar{P}_k(Fo)$  of other parameters  $P$  that define the evaporation process [12]. In the initial stage of evaporation, the droplet is warming up intensively and the temperature difference between the droplet surface and its surrounding gases decreases, therefore, the heat flux  $q_k^+$  slightly decreases. Then it starts to grow sequentially as the warming of the droplet weakens and the evaporation accelerates. The heating intensity of the liquid in the conductively heated droplet is defined by the density of the heat conduction flux on the inner surface of the droplet:  $q_{h,k} \equiv q_k^-$ , and in the case of combined heating – by the total heat flux density:  $q_{h,k+r} \equiv q_k^- + q_r$ .

The intensity of droplet evaporation can be described based on the heat flux caused by phase transformation, expressed through the total heat flux on the droplet surface. Assuming  $q_r^- = q_r^+ \equiv q_r$ ,

$$q_f = \bar{q}_s^+ + \bar{q}_s^- \equiv q_k^+ - \lambda \left. \frac{\partial T(r, \tau)}{\partial r} \right|_{r=R^-} \quad (3)$$

Eq. (3) shows the substantial influence of the temperature gradient on the droplet evaporation. When the gradient of the temperature field is positive, the absorbed radiation heat flux only warms the liquid of the droplet. When the gradient of the temperature field is negative, the absorbed radiation heat flux influences the evaporation of the droplet. Regardless of the heating method of the droplet, the conduction heat flux density of the droplet  $q_k^-$  decreases consistently. When the droplets are conductively heated by a gas of a higher temperature than the droplet itself, the heat flux density  $q_k^-$  becomes zero at the moment of the beginning of equilibrium evaporation and re-mains the

same until the droplet evaporates [12]. In the case of combined heating the density of the conductive heat flux in the droplet becomes zero as the negative temperature field gradient is formed, after which the density of the conductive heat flux in the droplet begins to increase again (Fig. 2). Its vector direction is already changed as is the nature of the heat flux energy origin: while previously the vector matches the conductive part of the heat flux from gas heating the liquid in the droplet, after the equilibrium evaporation process starts, it reflects the involvement in evaporation of the radiation flux absorbed in the droplet

$$\left. \begin{aligned} q_k^- &= q_k^+ - q_f, \text{ when } \left. \frac{\partial T(r, \tau)}{\partial r} \right|_{r=R^-} > 0 \\ q_k^- &\equiv q_f - q_k^+, \text{ when } \left. \frac{\partial T(r, \tau)}{\partial r} \right|_{r=R^-} < 0 \end{aligned} \right\} \quad (4)$$

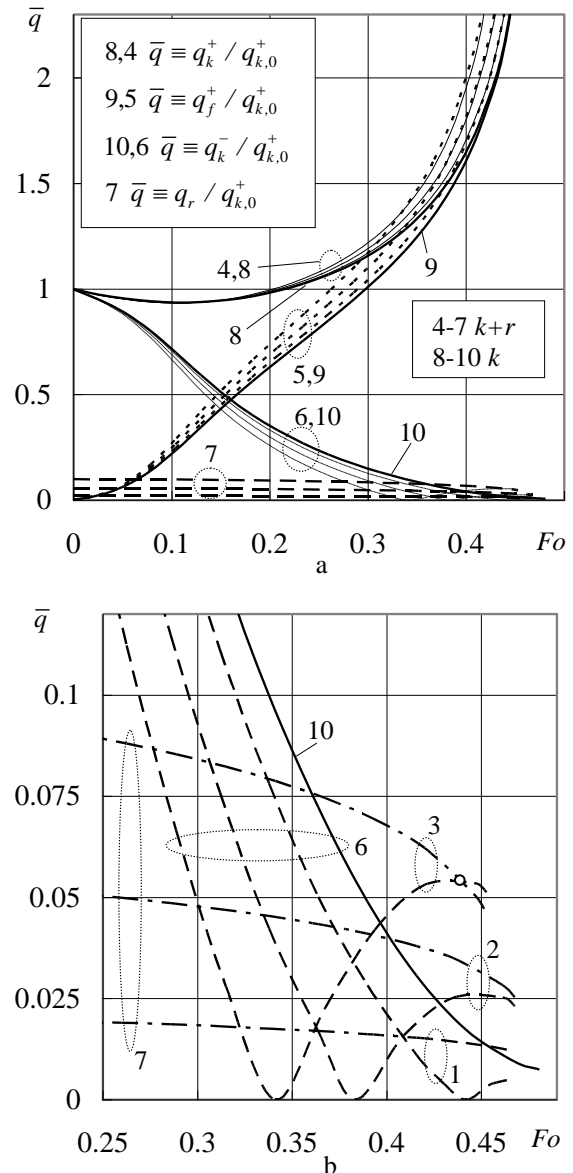


Fig. 2 The impact of radiation on the heat fluxes on the surface of the n-decane droplets: a - whole process of evaporation; b - final stage.  $R, m$ : 1 - 0.00005, 2 - 0.0001, 3 - 0.00015;  $q_{k,0}^+, kW/m^2$ : 1 - 593.04, 2 - 296.52, 3 - 197.38;  $T_g = 1000 K$

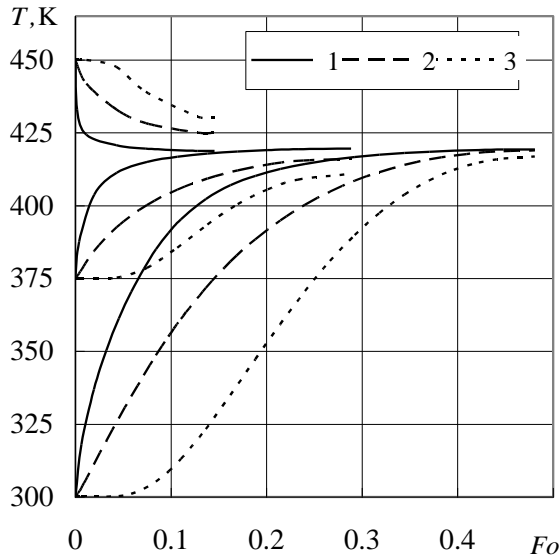


Fig. 3 The influence of initial temperature of sprayed n-decane on warming of evaporating droplets.  $T_g = 1000$  K

In the case of combined heating, equilibrium evaporation will only occur when the heat conduction flux value on the inside surface of the droplet becomes equal to the radiation flux absorbed by the droplet:  $q_{k,e}^- \equiv q_{r,e}$ . The energy state of the conductively heated droplets is of the same energy level and isothermal, so the temperature of equilibrium evaporation can be defined by the temperature of the droplet surface:  $T_{e,k} \equiv T_{R,e,k}$ .

Equilibrium evaporation of the droplets in the case of combined heating is possible when a negative gradient of temperature field is formed, ensuring that the conductive heat flux from the droplet will be able to remove absorbed radiative heat flux. The temperature field is individual for the droplets of different diameters, thus in the case of combined heating the equilibrium evaporation temperature can be defined only by the droplet average mass temperature:  $T_{e,k+r} \equiv T_{R,e,k+r}$ . The average mass temperature will not only be higher than the temperature  $T_{e,k}$  observed in the case of conductive heating, but also individual for the droplets of different sizes. Equilibrium evaporation temperature  $T_e$  does not depend on the sprayed liquid temperature: a lower temperature droplets warm to a temperature of  $T_e$ , a higher temperature droplets cool to a temperature of  $T_e$  (Fig. 3).

It is obvious that the droplets of n-decane usually do not reach the temperature of equilibrium evaporation, regardless of the initial temperature of the liquid in the droplet. The evaporation of n-decane differs distinctively from the well-known case of water droplet evaporation [8], in which nonstationary evaporation only takes about 20 percent of total evaporation time. This figure is exceeded by all n-decane droplets with initial temperature which deviates significantly from the droplet equilibrium evaporation temperature. In the modelled cases, internal layers of the conductively heated droplets do not reach isothermal conditions  $T_{e,k}(r) \equiv T_{R,e,k}$  which are necessary to begin equilibrium evaporation. In the case of combined heating only n-decane droplets with the diameter of 150 micrometres and an initial 300 K temperature reach thermal conditions needed to ensure equilibrium evaporation (Fig. 2, b).

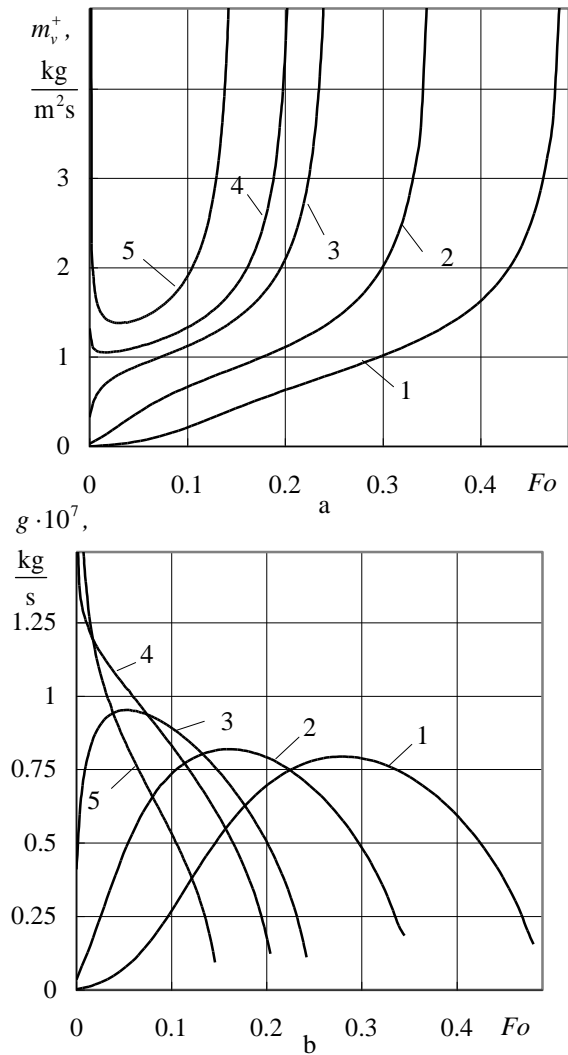


Fig. 4 The influence of the initial n-decane temperature on the evaporation of the conductively heated droplet mass: a - rate, b - flux.  $T_0$ , K: 1 - 300, 2 - 350, 3 - 400, 4 - 425, 5 - 450;  $T_g = 1000$  K;  $R_0 = 0.0001$  m

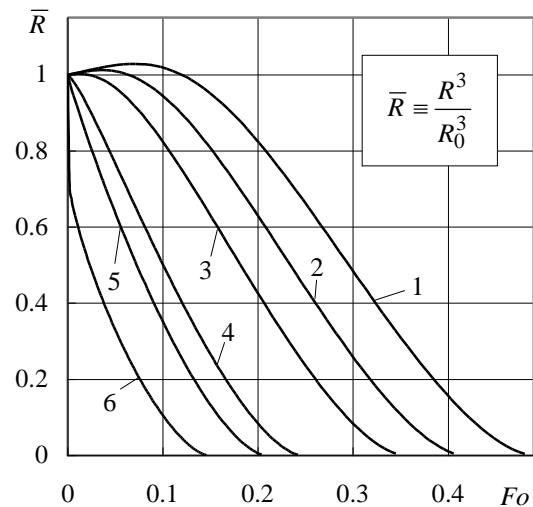


Fig. 5 The influence of the initial n-decane temperature on the evaporation speed of the conductively heated droplet.  $T_0$ , K: 1 - 300, 2 - 325, 3 - 350, 4 - 400, 5 - 425, 6 - 450;  $T_g = 1000$  K;  $R_0 = 0.0001$  m

The beginning of equilibrium evaporation is reflected by the intersection point between the curves that show radiation flux absorbed by the droplet and the curves that show heat conduction flux inside the droplet (Fig. 2, a).

The thermal state of equilibrium evaporation of the conductively heated n-decane droplet can be reflected by the temperature  $T_{R,e,k}$ . This temperature depends on the temperature and pressure of the surrounding gas: This function is very important for the energy assessment of the temperature of sprayed liquid impact on the droplet evaporation parameters.

When the pressure of the surrounding gas does not change, temperature  $T_{R,e,k}$  depends only on the temperature of the gas. Phase transformations on the surface of the droplet are directly influenced by heat fluxes affected by peculiarities of the warming of the n-decane droplets.

Influence of the initial temperature on the evaporation rate of the sprayed liquid droplets is shown in Fig. 4.

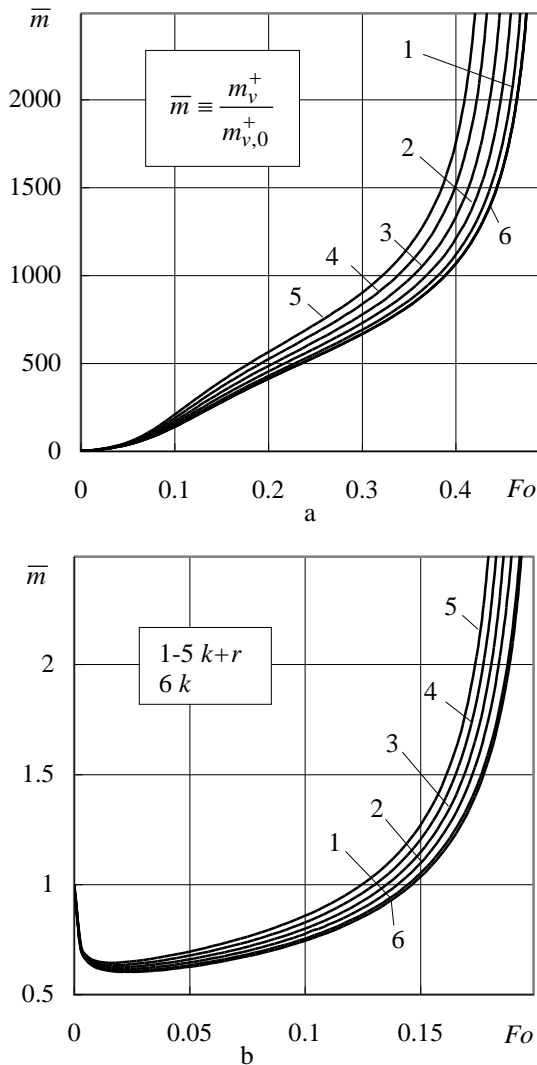


Fig. 6 The influence of heat radiation on evaporation intensity of the n-decane droplet: a - the case of "cold" liquid, where  $T_0 = 300$  K;  $m_{v,0}^+$ , kg/m<sup>2</sup>s: 1 - 0.00305, 2 - 0.00153, 3 - 0.00101, 4 - 0.00076, 5 - 0.00061; b - the case of "hot" liquid, where  $T_0 = 425$  K;  $m_{v,0}^+$ , kg/m<sup>2</sup>s: 1 - 3.681, 2 - 1.841, 3 - 1.227, 4 - 0.9204, 5 - 0.7363.  $T_g = 1000$  K;  $R$ , m: 1 - 0.00005, 2 - 0.0001, 3 - 0.00015, 4 - 0.0002, 5 - 0.00025

When temperature of the droplet is below  $T_{R,e,k}$ , the intensity of evaporation grows consistently, but when the temperature is higher - at the beginning the intensity of evaporation rapidly decreases, and only after that it begins to grow (Fig. 4, a). Meanwhile, the evaporation rate of "hot" droplets steadily decreases, while the evaporation rate of "cold" droplets grows in the beginning and only afterwards it begins to decrease (Fig. 4, b).

These evaporation intensity variation peculiarities together with the thermal expansion effect leads to volume changes of the n-decane droplet (Fig. 5).

The volume of "hot" droplets of n-decane decreases consistently and sharply due to the intensive evaporation and cooling fluid shrinkage effects. The expansion of liquid in the "cold" n-decane droplets in the phase of intensive warming compensates slow droplet evaporation and at the beginning of the process droplet volume grows (Fig. 5). The volume of the droplet starts to decrease when the evaporation of the droplet begins to dominate against the expansion of the liquid. Peak point of curve  $\bar{R}(Fo)$  shows the moment of equilibrium between the warming liquid expansion and the liquid droplet evaporation processes.

In the final stage of phase transitions the intensity of "cold" droplet evaporation increases several thousand times compared to the initial intensity of evaporation (Fig. 6, a). Meanwhile, the "hot" droplet evaporation intensity decreases first and only after that increases just a few times (Fig. 6, b). However, it should be noted that the initial evaporation of "hot" n-decane droplet is several thousand times more intensive: for modelled droplet with the initial diameter of 100 micrometers it is a 3.681 kg/m<sup>2</sup>s, and for "cold" as low as 0.00305 kg/m<sup>2</sup>s. The process of droplet evaporation is also affected by heat radiation from the surroundings of the droplet.

The heat radiation flux from the surroundings of the droplet affects "cold" (Fig. 6, a) and "hot" (Fig. 6, b) n-decane droplet evaporation differently: evaporation of "cold" n-decane droplet is accelerates more intensively.

#### 4. Conclusions

When temperature and pressure of the gas surrounding the droplet and the initial temperature of the conductively heated droplet is defined, the change of sprayed liquid dispersion causes a proportional change of heat fluxes of different nature on the surface of the droplet. This, in turn, is the physical preconditions for similarity of other parameters that are influenced by the heat flux and independent from the size of the droplet. Therefore, the variation of the aforementioned heat fluxes after normalization is identical regardless of the diameter of the droplets in the  $Fo$  time scale.

The influence of combined heating on the evaporation of dispersed liquid can be assessed by evaluating the deviation of the heat and mass transfer parameters relative to the characteristic curves of conductive heating.

The research showed a substantial influence of the initial temperature of the dispersed n-decane droplets on the thermal state transitions and the rate of evaporation.

The significantly higher evaporation rate of "hot" n-decane droplets can be explained by a significant contribution of the internal energy to the droplet energy balance.

## References

1. <http://www.sciencedirect.com/> (2012-01-30)
2. **Semenov, S.; Starov, V.M.; Velarde, M.G.** 2011. Droplets evaporation: Problems and solution, Eur. Phys. J. Special Topic 197: 265-278. <http://dx.doi.org/10.1140/epjst/e2011-01468-1>.
3. **Moriue, O.; Eigenbrod, C.; Rath, H.J.; Sato, J.; Okai, K.; Tsue, M.; Kono, M.** 2000. Effects of dilution by aromatic hydrocarbons on staged ignition behaviour of n-decane droplets, Proceedings of the Combustion Institute 28: 969-975. [http://dx.doi.org/10.1016/S0082-0784\(00\)80303-3](http://dx.doi.org/10.1016/S0082-0784(00)80303-3).
4. **Miliauskas, G.; Sinkunas, S.; Talubinskas, J.; Sinkunas, K.** 2010. Peculiarities of hydrodynamics in the evaporation of hydrocarbon droplets, Advances in Fluid Mechanics VIII: WIT Transactions on Engineering Sciences 69, Boston, 283-292.
5. **Sazhin, S.S.** 2006. Advanced models of fuel droplet heating and evaporation, Progress in Energy and Combustion Science 32: 162-214. <http://dx.doi.org/10.1016/j.pecs.2005.11.001>.
6. **Dombrovskii, L.A.; Sazhin, S.S.** 2003. A simplified non-isothermal model for droplet heating and evaporation, Int. Comm. Heat Mass Transfer 30: 787-796. [http://dx.doi.org/10.1016/S0735-1933\(03\)00126-X](http://dx.doi.org/10.1016/S0735-1933(03)00126-X).
7. **Sazhin, S.** 2005. Modeling of heating, evaporation and ignition of fuel droplets: combined analytical, asymptotic and numerical analysis, J. of Physics: Conference Series 22: 174-193.
8. **Miliauskas, G.** 2001. Regularities of unsteady radiative-conductive heat transfer in evaporating semitransparent liquid droplets, Int. J. Heat Mass Transfer 44: 785-798. [http://dx.doi.org/10.1016/S0017-9310\(00\)00127-7](http://dx.doi.org/10.1016/S0017-9310(00)00127-7).
9. **Miliauskas, G.; Garmus, V.** 2009. The peculiarities of hot liquid droplets heating and, Int. J. Heat Mass Transfer 52: 3726-3737. <http://dx.doi.org/10.1016/j.ijheatmasstransfer.2009.03.001>.
10. **Liu, Y.; Yang, J.; Qin, J.; Zhu, A.** 2012. Heat transfer for film condensation of vapour, Mechanika 18(1): 56-62.
11. **Vaidelienė, A.; Vaidelys V.** 2012. Air bubbles and water droplets entrainment and removal in turbulent-water flows, Mechanika 18(1): 63-67.
12. **Miliauskas, G.; Sabanas, V.; Bankauskas, R.; Miliauskas, G.; Sankauskaite, V.** 2008. The peculiarities of sprayed liquid's thermal state change, as droplets are heated by conduction, Int. J. of Heat and Mass Transfer 51: 4145-4160. <http://dx.doi.org/10.1016/j.ijheatmasstransfer.2008.01.016>.
13. **Tuntomo, A.; Tien, C.L.** 1992. Optical constant of liquid hydrocarbon fuels, Combust. Sci. and Tech. 84: 133-140. <http://dx.doi.org/10.1080/00102209208951849>.
14. **Kuzikovskij, A.V.** 1970. Dynamic of spherical particle in optical field Izv. VUZ Fizika 5: 89-94 (in Russian).

G. Miliauskas, J. Talubinskas, A. Adomavičius, E. Puida

GARUOJANČIŲ ANGLIAVANDENILIO LAŠELIŲ TERMINĖ BŪSENA IR HIDRODINAMIKA.  
2. IŠPURKŠTO N-DEKANO GARAVIMO PROCESO ENERGINĖ INTERPRETACIJA

### Re z i u m ė

Straipsnyje pateikti išpurkšto angliavandnenilio n-dekano lašų garavimo procesų skaitinio tyrimo rezultatai. Šildymo laidumu atveju išnagrinėti garavimo metu pasireiškiantys šilumos srautai lašelio paviršiuje. Juos sunormavus ir atvaizdavus Furjė laiko koordinatėse, gautos būdingos kreivės, nepriklausančios nuo pradinio lašelio skersmens. Tiriant lašelio pradinės temperatūros, aplinkos šiluminio spinduliavimo įtaką, nustatyta pusiausviros garavimo būsenos galimybė, garavimo greičio, intensyvumo kitimas garavimo proceso metu. Energinė analizė išryškino garavimo proceso ypatybes, sąlygojamas skirtingos prigimties energijos srautų sąveikos.

G. Miliauskas, J. Talubinskas, A. Adomavičius, E. Puida

THE THERMAL STATE AND HYDRODYNAMICS OF EVAPORATING HYDROCARBON DROPLETS.  
2. ENERGY INTERPRETATION OF SPRAYED N-DECANE EVAPORATION PROCESS

### S u m m a r y

This paper presents the results of a numerical investigation of sprayed hydrocarbon n-decane droplets evaporation processes. For the case of conductive heating heat fluxes on the surface of the evaporating droplet were examined. Characteristic curves unrelated to the initial droplet diameter were obtained after the aforementioned heat fluxes were normalized and displayed in Fourier time coordinates. The influence of initial droplet temperature and surrounding thermal radiation was investigated. As a result of this investigation, the possibility of the equilibrium evaporation state, evaporation rate and intensity changes during the process of evaporation were evaluated. In the result of energy interpretation of interaction between heat fluxes of different nature the characteristics of the process of evaporation were highlighted.

**Keywords:** n-decane, evaporation, combined heating.

Received June 03, 2011

Accepted June 13, 2012